THE JOURNAL OF PHYSICAL CHEMISTRY B

Article

pubs.acs.org/JPCB

Bottom-Up Approach to Eumelanin Photoprotection: Emission Dynamics in Parallel Sets of Water-Soluble 5,6-Dihydroxyindole-Based Model Systems

Alice Corani,[†] Annemarie Huijser,[†,⊥] Alfonso Iadonisi,[‡] Alessandro Pezzella,*[,‡] Villy Sundström,[†] and Marco d'Ischia[‡]

[†]Department of Chemical Physics, Lund University, Box 124, 221 00 Lund, Sweden

[‡]Department of Chemical Sciences, University of Naples "Federico II", Via Cintia, 80126 Naples, Italy

Supporting Information

ABSTRACT: The molecular mechanisms by which the black eumelanin biopolymers exert their photoprotective action on human skin and eyes are still poorly understood, owing to critical insolubility and structural heterogeneity issues hindering direct investigation of excitation and emission behavior. Recently, we set up strategies to obtain water-soluble 5,6-dihydroxyindole (DHI)-based polymers as useful models for disentangling intrinsic photophysical properties of eumelanin components from aggregation and scattering effects. Herein, we report the absorption properties and ultrafast emission dynamics of two separate sets of DHI-based monomer−dimer−polymer systems which were made water-soluble by means of poly(vinyl alcohol) or by galactosyl-thio substitution. Data showed that dimerization and polymerization of DHI result in long-lived excited states with profoundly altered properties relative to the monomer and that glycosylation of DHI imparts monomer-like behavior to oligomers and polymers, due to steric effects hindering planar conformations and efficient interunit electron communication. The potential of S-glycation as an effective tool to probe and control emission characteristics of eumelanin-like polymers is disclosed.

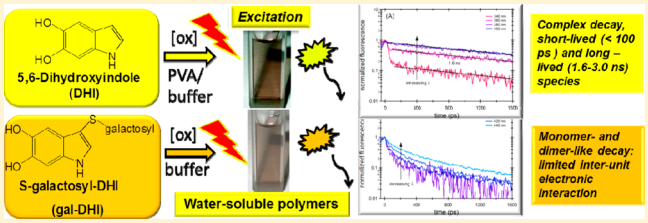

INTRODUCTION

A heavily pigmented skin with high levels of eumelanins, the black insoluble biopolymers produced by cutaneous melanocytes,[1−3] is commonly believed to indicate an efficient protection against the damaging effects of intensive or chronic sun exposure and a lower susceptibility to melanoma and other aggressive forms of skin cancer. Besides the role in photoprotection,[1,3,4] melanogenesis itself has been investigated as a targeting strategy against melanoma growth.[5] Biosynthetically, eumelanins arise within organelles termed melanosomes by tyrosinase-catalyzed oxidation of tyrosine via oxidative polymerization of 5,6-dihydroxyindole (DHI), 5,6-dihydroxyindole-2-carboxylic acid (DHICA), and other biosynthetic intermediates (Scheme 1).[1]

The oxidative polymerization process involves the generation of extremely complex mixtures of oligomeric species at various levels of oxidation and degrees of polymerization, linked through diverse bonding patterns[7] depending on the nature of the precursors[6,8−10] and featuring apparent molecular weights up to 4000 amu.[11] As polymerization proceeds, aggregation processes and deposition of black insoluble particles within the melanosomes become significant and concur to determine the complex supramolecular organization of eumelanin biopolymers.[12]

Similar phenomena occur also in model processes of eumelanin buildup involving biomimetic oxidation of DHI and related metabolites: in all cases dark insoluble polymers are produced which share free radical and optoelectronic characteristics in common with natural eumelanins despite different morphological and surface properties.[13]

Although a huge body of epidemiological and biological data supports the superior adaptation of dark-skinned individuals to outdoor lifestyles in sunny areas, the precise mechanisms underlying eumelanin's photoprotective role, including the intrinsic structural factors that govern broad-band absorption features (the "black" chromophore) and relaxation pathways from the monomer to polymer range, remain poorly understood. Elucidation of the photoprotective mechanisms of eumelanin biopolymers is hindered mainly by the marked insolubility in most solvents, with aggregation phenomena and scattering effects compounding significantly mechanistic analysis, and the extreme molecular heterogeneity, reflecting the lack of an ordered and well-characterized molecular structure.

Purportedly, eumelanins afford photoprotection by way of their unique photophysical properties, including broad-band absorbance coupled with very low emission (<0.1%) reflecting the ability to efficiently transfer excitation energy into chemical

Received: June 29, 2012
Revised: October 12, 2012
Published: October 16, 2012

Scheme 1. Scheme Showing a Simplified Mechanism of Natural Eumelanin Buildup via Initial Oligomer Growth from Oxidative Polymerization of DHI[6−8] and DHICA[9,10] (Mixed Oligomers Are Not Shown for the Sake of Simplicity) Followed by Aggregate Formation and Particle Separation

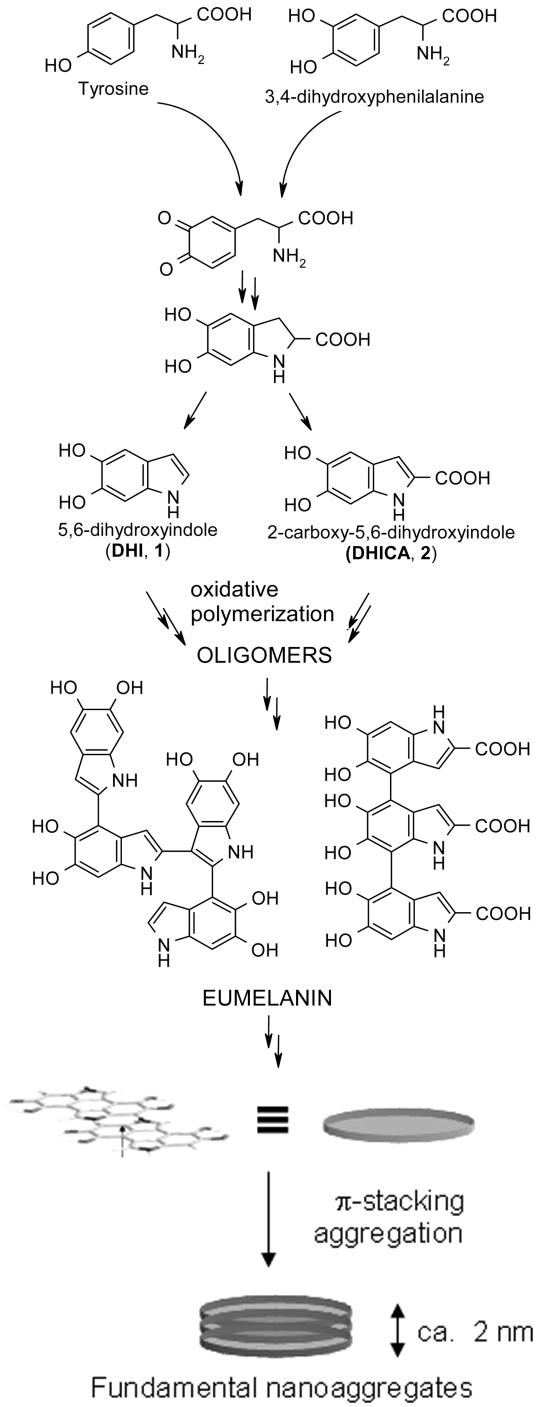

energy.[14,15] Approximately 99.9% of the UV energy absorbed by eumelanin dissipates as heat on a time scale of <1 ns[16] raising intriguing issues about the nature of the major deactivation channels.[2] Although the UV−visible absorption characteristics of DHI and its oligomers have been investigated to some extent,[15,17−21] no clear-cut relationship between spectral properties of the oligomer structures and the cross sections of the monomeric building blocks has been defined, since the spectroscopic properties of the oligomers vary in a complex and not entirely predictable manner with the bonding patterns between units.[4,12]

Investigation of eumelanin emissive properties is even more challenging due to strong fluorescence quenching. Main difficulties derive from the variable broad-band absorption profiles of eumelanins, affecting comparison of data from different samples, and from intra- and intermolecular coupling, introducing fast excited state deactivation channels amplified in the heterogeneous supramolecular systems. It is therefore not uncommon to find reports in which it is stated that eumelanins do not fluoresce at all.[15,18]

Accurate measurements of fluorescence properties of synthetic eumelanin solutions revealed a single broad emission band[22] attributed to a combination of different narrower peaks reflecting the fluorescence of the different species that constitute the macromolecular eumelanin ensemble.[18] In line with this view was the strong excitation wavelength dependence observed in those studies, supporting interpretation of fluorescence features in terms of the selective excitation of different-sized oligomers. The detailed mechanisms accounting for the relatively small radiative quantum yields of eumelanins are still obscure, and various hypotheses have been put forward. It is likely that diverse concurring factors, including strong intra- and intermolecular coupling (as well as water coupling), contribute to efficient excited state quenching, leading ultimately to nearly quantitative nonradiative conversion of absorbed photons.[22,23] Efficient emission reabsorption has been indicated as one of the main factors altering the emission spectra and hindering studies of emission dynamics. This was apparent from experiments in which the photophysical properties of eumelanin were investigated introducing a correction to excitation spectra to account for absorption effects and reconstruct the excitation profiles.[22] Thus, although complex multiexponential fluorescence decay profiles have been observed for eumelanins, the dependence of the emission dynamics on excitation and emission wavelength has remained not well understood.

The dynamics of radiative relaxation in eumelanin have been studied using traditional picosecond time-resolved fluorescence techniques.[24,25] Other insights have been gained via investigations of two-photon effects[26,27] and by a photoacoustic study.[28]

State-of-the-art, time-dependent, density functional theory calculations of the relaxation dynamics of eumelanin model indolic oligomers suggest that after excitation ultrafast energy conversion takes place through two main mechanisms: proton transfer on a time scale of 110 fs and state mixing upon oligomerization on a time scale of <50 fs.[29] The time scale for state mixing was predicted to be very sensitive to the extent of polymerization: whereas monomers do not show significant state mixing, dimers show state mixing on a 50 fs time scale, and tetramers on an even shorter time scale of 30−40 fs. Thus, calculations suggest that the overall nonradiative relaxation in eumelanin building blocks takes place within a time <50 fs through state mixing and proton transfer, in apparent agreement with the transient absorption data recorded by femtosecond pump−probe experiments.[30] Yet, despite these and other advances, current understanding of the UV dissipation mechanisms and especially the radiative pathways has remained limited. Herein, we report a new approach to elucidate eumelanin fluorescence properties and dynamics

which capitalizes on the recent development of water-soluble 5,6-dihydroxyindole polymers novel efficient experimental tools. The main objective of the study was to attempt to disentangle the intrinsic photophysical properties of eumelanin model constituents under conditions in which heterogeneity and insolubility issues are circumvented, in order to provide novel conceptual and methodological tools in the current pursuit of photoprotection mechanisms. We find that at the monomer level excited state species and dynamics are qualitatively similar under all conditions, demonstrating the usefulness of the solubilization approaches. Excitation to a high-lying excited state (S_4)[31] results in formation of a radical with short excited state lifetime, whereas the lowest S_1 excited state has a long nanosecond lifetime.[31−33] Coupling of two DHI units within biindole scaffolds drastically changes the photochemistry and eliminates the radical formation channel observed in monomers. Solubilization using a glycation strategy[21] introduces steric hindrance, decreasing intramolecular interunit interactions into dimers and polymers and recovering partial monomer-like behavior. Overall, the results show that under most conditions DHI-derived species, including dimers and polymers, form long-lived excited states and radical species as a result of UV absorption. This could have important implications for our understanding of DHI-pigment-related phototoxicity.

EXPERIMENTAL SECTION

Samples. 5,6-Diacetoxyindole, 5,6-diacetoxyindol-3-yl-1-thio-β-D-galactopyranoside, and related dimers were prepared according to the literature.[34,21] Samples were >99% pure as judged by proton NMR analysis at 400 MHz using DMSO-d_6 as the solvent. Spectra were obtained by averaging up to 1000 scans on samples at 0.2 M concentration (purity grade above 99%).

Deacetylation of 5,6-Dihydroxyindole Derivatives. Acetylated eumelanin precursors (60 mg, 0.10 mmol) were treated with sodium *tert*-butoxide in MeOH (2 mL) under nitrogen atmosphere for 1 min to achieve complete deacetylation (NMR and MS evidence). The mixture was then diluted with 0.1 M phosphate buffer, pH 7.0 (10 mL) for in situ oxidative polymerization.

Synthetic Melanin Preparation. Oxidation of the appropriate substrate (12.5 mM) in 0.1 M phosphate buffer pH 7.0 was carried out with horseradish peroxidase (HRP, 25 U/ml) and H_2O_2 (12.5 mM).[9] After 20 min the solution was diluted 25−100-fold with 0.1 M phosphate buffer pH 7.0 for optical characterization. Poly(vinyl alcohol) (PVA)-containing buffer was prepared by dissolving PVA in phosphate buffer in the appropriate weight ratio and warming to prevent cluster formation. PVA-containing buffers were thermostatted at the desired temperature prior to use. When necessary, the mixture was treated with a solution of $NaBH_4$ in methanol (20 mM).

Steady-State Optical Characterization. Absorption spectra were measured by using an Agilent spectrophotometer. Steady-state fluorescence spectra were recorded with excitation at 280 nm using a spectrofluorometer (Spex, Fluorolog).

Fluorescence Streak Camera Experiments and Data Analysis. Infrared pulses with a central wavelength of 840 nm, a pulse duration of 100 fs, and a repetition rate of 82 MHz (Spectra-Physics, Tsunami) were frequency-tripled using a harmonic generator (Photop Technologies, Tripler TP-2000B). Pulses with a pulse energy of 1−5 pJ and central wavelength of 280 nm were focused on the sample using a 100 mm focal length quartz lens. The sample solution was kept in a quartz rotating cuvette with an optical path length of 2 mm and had an optical density at 280 nm of 0.2, corresponding to concentrations on the order of 0.03 mM. For optical densities at 280 nm of 0.2 and lower, no concentration dependence of the excited state dynamics was observed. The fluorescence was collected at magic angle polarization using two 1 in. 50 mm focal length quartz plano-convex lenses and focused on the input slit of a spectrograph (Chromex) with 50 lines/mm, blazed at 600 nm. The output of the spectrograph was sent into a streak camera setup (Hamamatsu C6860), which was operated with a slit width of 100 μm giving a temporal response function of ∼50 ps at the time window used (time range 6). Experimental data were corrected for background and shading. Significant chemical degradation due to illumination was excluded on basis of similar optical density spectra before and after the measurements. In a range of 0.2−5 pJ per pulse, no intensity dependence of the excited state dynamics was observed. The contribution originating from the PVA was negligible. Global fit analysis was perfomed on the time-resolved data, using either Matlab or Igor software. A single- or biexponential model was used to extract the rate constants without fixed time intervals.

RESULTS AND DISCUSSION

Sample Preparation Issues and Experimental Design. As reported previously, several obstacles have hindered attempts to elucidate the photophysical and chemical properties and excited state dynamics of both natural and synthetic eumelanins. Main difficulties arise from the marked chemical heterogeneity and insolubility of eumelanins in all solvents[5] and the lack of standardized preparation protocols for synthetic eumelanins, which usually account for poorly reproducible and incomparable data from one sample to the other. In addition, several reports refer to commercial alkali-soluble polymers[35−37] derived from tyrosine and hydrogen peroxide, whose structural relationship with insoluble natural or synthetic polymers is unknown and questionable.

Accordingly, the present study was designed to address two of the main problems hindering elucidation of the intrinsinc photophysics of eumelanin constituents: chemical heterogeneity and insolubility. Issues relating to chemical heterogeneity were circumvented by employing as precursors the ultimate monomer intermediate in the biosynthetic pathway, DHI or a derivative, which give on oxidation only mixtures of oligomer species homogeneous with regard to monomer composition.

Solubility problems, on the other hand, have been circumvented by integrating two recently developed strategies for studying eumelanin black chromophore in aqueous solution. These strategies involve oxidative polymerization of (a) DHI in the presence of poly(vinyl alcohol) (PVA), which can prevent oligomer aggregation and precipitation,[38] and (b) an *S*-galactosylthio-DHI (gal-DHI) derivative, which yields a dark soluble polymer.[21] In the gal-DHI monomer and its oxidation products, the sulfur atom on the 3-position provides a flexible bridge linking the indole unit to the sugar moiety without affecting significantly the mode of polymerization of the unit DHI, as demonstrated previously.[7,21] It should be noted that the 3-position is relatively little involved in the oxidative polymerization of DHI, so that the sulfur substituent is not expected to affect the eumelanin-like character of the resulting polymers. Furthermore, the sulfur center provides a useful

mechanistic tool to probe photophysical and photochemical processes involving the indole ring.

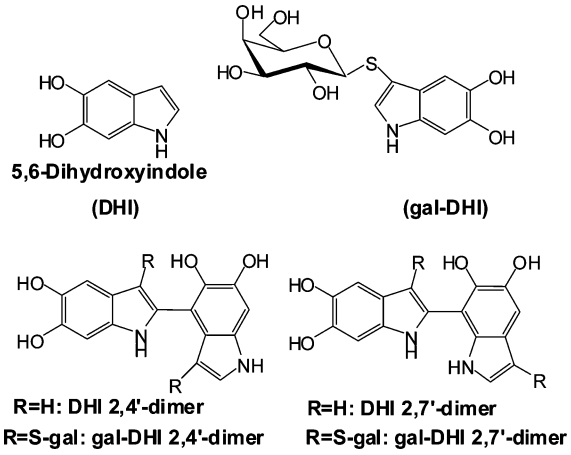

Figure 1. 5,6-Dihydroxyindole derivatives used as substrates in this study.

Besides water solubility and use of homo dimers/polymers, an additional strength of the present approach is the comparative perspective that emerges from studies of two different monomer−dimer−polymer sets belonging to the PVA-added and S-glycated series.

Comparison of data from monomers and dimers was aimed to gain information about structural effects related to unit−unit coupling, electron delocalization, and molecular size effects, whereas investigation of polymers introduced the role of unit oxidation and the presence of quinones.[21,38−40] It is worth mentioning here that within eumelanin-type polymers, reduced (catechol) and oxidized (quinonoid) moieties coexist and would sustain stacking intermolecular interactions possibly associated with charge transfer.

Comparison of data from the two series (S-glycated and PVA-solubilized) was directed to probe the differential susceptibility of the various electronic transitions and excited state dynamics in DHI to structural effects related to the sulfur atom and conformational bias by the bulky sugar groups.

Steady-State Absorption and Fluorescence of Monomers, Dimers, and Eumelanin-Type Polymers. The absorption spectra of monomers, dimers, and polymers have been described previously and are therefore only shown in the Supporting Information. Steady-state fluorescence spectra are shown in Figure 2. Samples were excited at 280 nm, the same excitation wavelength as used for recording the time-resolved fluorescence data..

The DHI monomer shows a strong fluorescence band around 330 nm and a less intense shoulder around 380 nm, both in buffer and in PVA-containing buffer. It has been shown previously that the 330 nm fluorescence band is due to emission from the DHI cation radical (or its neutral radical), generated from the S_4 excited[31] state. The 380 nm band is due to fluorescence from the lowest S_1 excited state of DHI. Substitution with the *S*-galactosyl group resulted in a bathochromic shift with a concomitant increase of the low-energy band and an apparent weakening of the high-energy band. The lower intensity of the 330 nm band in gal-DHI suggests that there is a less efficient radical formation in this DHI derivative as compared to parent DHI. The red-shift of the low-energy fluorescence band upon gal-S derivatization can possibly be ascribed to the influence of the sulfur atom (see also below).

For the DHI dimers, the main change relative to the monomer is the disappearance of the 330 nm band and a small red-shift to ∼390 nm of the low-energy fluorescence band. . The disappearance of the 330 nm fluorescence band and the red-shift of the low-energy band of the DHI dimers can tentatively be attributed to absence of the radical formation channel and interunit electron delocalization, respectively. The same trend is noticed along the gal-DHI series, where the monomer band at 330 nm is lacking and the low-energy band shifts to about 410 and 420 nm for the 2,7′- (Figure 2B) and 2,4′- (Figure S5, Supporting Information) dimers, respectively. Moreover, the 2,4′-dimer of gal-DHI exhibits very weak fluorescence. The red-shift of the low-energy band of the gal-S dimers probably has a similar origin as the corresponding shift of the gal-DHI monomer. Comparison of absorption and fluorescence spectra between DHI dimers and the glycated derivatives reveals an interesting difference: whereas the gal-S substituent shifts emission toward longer wavelengths, it causes an opposite effect on the main absorption bands. The latter effect likely reflects steric hindrance of the bulky sugar groups inhibiting coplanar conformations, leading to lower interunit electron delocalization with respect to the unsubstituted biindoles.

Overall these data disclose different susceptibility of the DHI fluorescence bands to structural factors: in particular, the high-energy band is decreased by both dimerization and sulfur substitution at the 3-position (possibly due to decreased radical

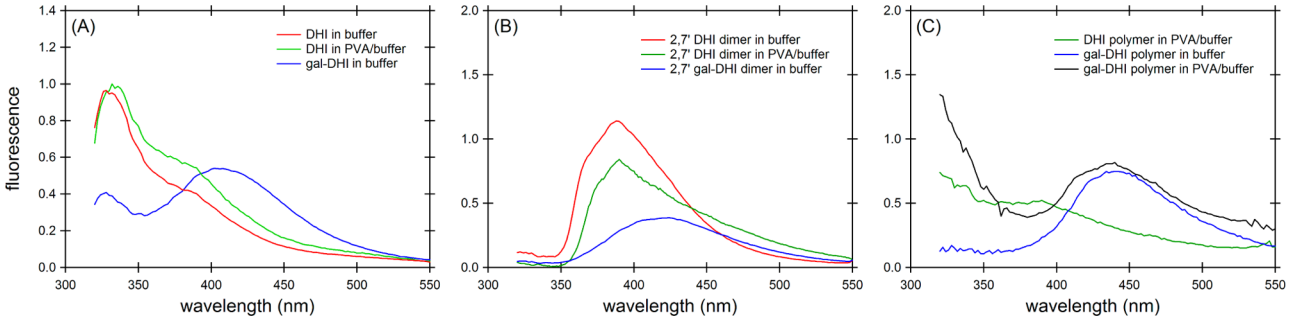

Figure 2. Steady-state fluorescence spectra of the studied (A) monomers: red line, DHI in buffer; green line, DHI in PVA/buffer; blue line, gal-DHI in buffer, (B) dimers: red line, 2,7′ DHI dimer in buffer (the spectrum for the 2,4′-dimer is shown in the Supporting Information); green line, 2,7′ DHI dimer in PVA/buffer; blue line, 2,7′ gal-DHI dimer in buffer, and (C) polymers: green line, DHI polymer in buffer; black line, gal-DHI polymer in buffer; blue line, al-DHI polymer in PVA/buffer.

dx.doi.org/10.1021/jp306436f | *J. Phys. Chem. B* 2012, 116, 13151−13158

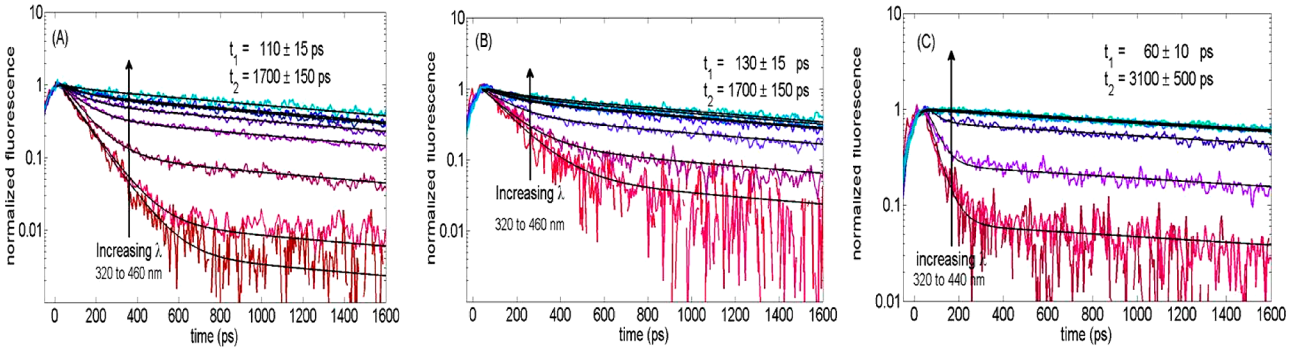

Figure 3. Fluorescence decay kinetics of DHI in buffer (A), DHI in PVA/buffer, (B) and gal-DHI in buffer (C), including fits using a biexponential decay function and the resulting lifetimes with corresponding amplitudes. The corresponding tables of the amplitudes for the two exponential components are reported in the Supporting Information.

formation), while the low-energy band becomes more intense. As expected, the fluorescence properties of the polymers are significantly altered, and the emission is markedly weakened. Interestingly, emission from the gal-DHI polymer is much more intense than from the DHI polymer in PVA/buffer and is shifted to longer wavelengths (ca. 440 vs 390 nm, Figure 2C). Moreover, within the glycated series, the emission from monomer to dimer is significantly shifted to longer wavelengths.

The fluorescence responses from the PVA-solubilized versus glycated DHI series showed similar trends although some observations deserve a comment. First, a very small difference is noted between spectra in buffer alone and in PVA-containing buffer, indicating that PVA does not affect to any significant extent the excitation and emission profiles of the indole species examined. It should be noted that the fluorescence intensity for the PVA-solubilized polymers at wavelengths shorter than 350 nm has contributions from scattered excitation light. It is concluded that PVA is a reliable and so far unique tool to dissect emission properties in pristine underivatized eumelanin building blocks and DHI polymers in the absence of aggregation and scattering effects.

Second, whereas the gal-S substituent in the glycated series affects only moderately absorption maxima and cross sections at the monomer and dimer levels, it exerts significant effects on the emission profiles, inducing an approximately 40 nm red-shift with band broadening. On this basis, it is proposed that the S-glycated substituent can be used as bifunctional probe, in which the sulfur perturbs the π-electron features of the indole, biindole, and polymer systems while the sugar moiety exerts steric effects over interunit dihedral angles in oligomer and polymer chains and controls aggregation and precipitation.

Third, a marked decrease in fluorescence intensity was observed within the parent indole series from the monomer/dimer to the polymer. This effect conceivably reflects the presence in the polymer of more or less delocalized quinonoid units, which would not emit significantly, thus altering the emission intensity. On this basis, it could be speculated that the fluorescence properties of eumelanin-like polymers are largely due to reduced monomer/oligomer moieties within constituent molecular species.

Fluorescence Decay Kinetics: Monomers. Figure 3 shows fluorescence decay kinetics of DHI in buffer (A), DHI in PVA/buffer (B), and gal-DHI in buffer (C). Fits using a biexponential decay function and the resulting lifetimes are given as insets. As described in detail in a previous papers, DHI either in buffer[31,33] or in PVA-containing buffer[31] shows dual fluorescence with lifetimes of 110 ps (in buffer solution; in PVA/buffer the lifetime is 130 ps) and 1.7 ns. The contribution of the 110 ps (130 ps) component increases with decreasing fluorescence wavelength while the opposite applies to the 1.7 ns decay. Thus for DHI in buffer, the decay at 320 nm is entirely due to the 110 ps component, whereas at 460 nm only the slow 1.7 ns decay is observed. A very similar behavior is observed for DHI in PVA/buffer (Figure 3 B). Shorter excitation wavelength also increases the relative contribution of the fast-decay component.[31,33] Most likely, the 110 ps decay is due to a DHI radical cation generated by electron transfer to the solvent from the highly energetic S_4 excited state (Figure 4).[31] This

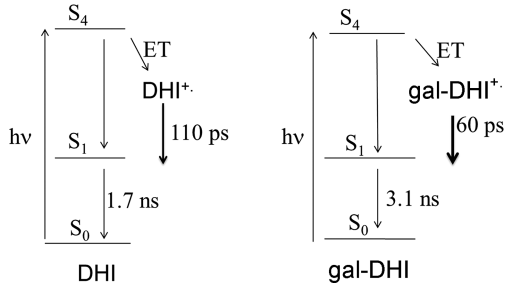

Figure 4. Diagram showing proposed excited state deactivation channels in DHI and gal-DHI (ET = electron transfer to solvent).

process is very fast (subpicosecond) and would compete with internal conversion from the S_4 to the S_1 state. Though DFT calculations show low oscillator strengths for the S_0-S_2 and S_0-S_3 transitions,[41] internal conversion from the S_4 to the S_1 state very likely occurs via the S_3 and S_2 states. It is possible that electron transfer to solvent is followed by a proton transfer step leading to an overall H-atom transfer, as recently proposed on the basis of quantum chemical calculations.[41] This latter event would yield a neutral radical rather than a radical cation as the photochemical product of UV absorption. The 1.7 ns lifetime represents the fluorescence decay of the lowest S_1 excited state of DHI.[31,33,42]

Compared to DHI, gal-DHI shows qualitatively similar, but quantitatively different, time-resolved properties. In particular, both fast and slow fluorescence decays are observed, but the fast component is now faster (~60 ps) and the slow is 3.1 ns, i.e., slower than that of the parent DHI. This difference indicates some alteration of excited state processes. Using the above assignments, it appears that the galactosylthio group

dx.doi.org/10.1021/jp306436f | J. Phys. Chem. B 2012, 116, 13151−13158

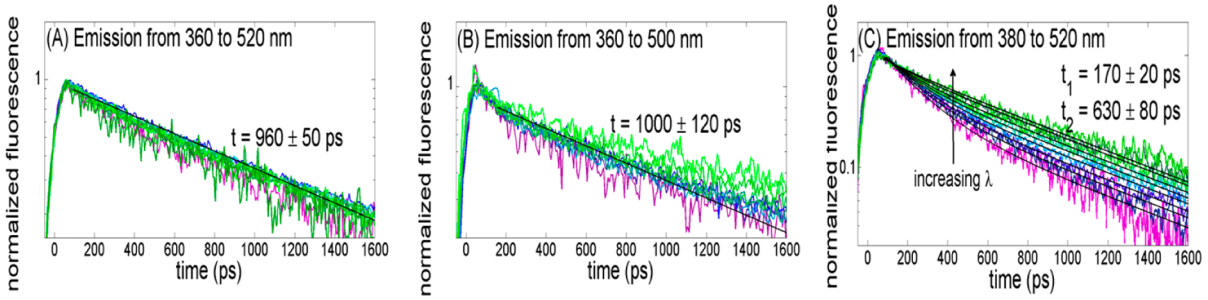

Figure 5. Fluorescence decay kinetics of the 2,7′ DHI dimer in buffer (A), the 2,7′ DHI dimer in PVA/buffer (B), and the gal-DHI, 2,7′-dimer in buffer (C), including fits using a mono- or biexponential decay function and the resulting lifetimes. The corresponding tables of the amplitudes for the two exponential components are reported in the Supporting Information.

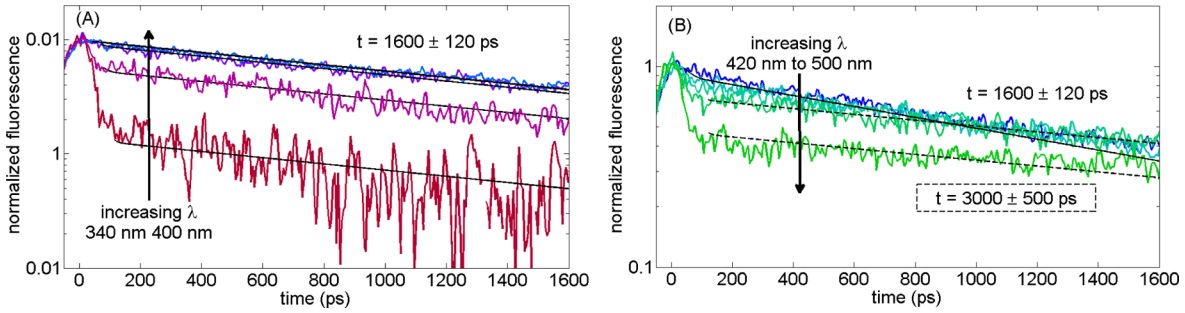

Figure 6. Fluorescence decay kinetics of the DHI polymer in PVA/buffer in the UV (A) and visible part of the emission spectrum (B), including fits to the slow monoexponential nanosecond decay and the resulting lifetimes. Lambda steps: 20 nm.

favors decay of the radical species and slows down deactivation of the low-energy excited state. Interestingly, it can be speculated that in gal-DHI in the S_4 state, electron transfer leads to a different radical species, probably via electron loss at the sulfur center, accounting for the different decay or recombination characteristics. On the contrary, a stabilizing effects of the sulfur atom on the S_1 state would cause emission at lower energy and slower decay kinetics.

Fluorescence Decay Kinetics: Dimers. Considerable changes in the excited state dynamics are observed on passing from monomers to dimers in both series as apparent from the fluorescence decays of the 2,7′-dimer series (Figure 5) and of the 2,4′- and 2,2′-dimers of DHI (see the Supporting Information). The fluorescence lifetimes were obtained from global analysis using a single- or biexponential decay function. For all three dimers, the nanosecond fluorescence lifetimes would entail relative excited state stability. Scrutiny of the data shows that the excited state decay of the 2,7′-dimer is characterized by a nearly monoexponential function independent of concentration and fluorescence wavelength, with a single major species having a lifetime of 960 ps. In the case of the 2,4′-dimer, the decay is apparently biexponential (Figure S6, Supporting Information), with time constants of 150 ps (minor component, 25%) and 1.5 ns (major component, 75%), and is independent of the wavelength, indicating a single emitting species. The fluorescence decay of the 2,2′-dimer is single exponential with a lifetime of 1350 ps (Figure S5, Supporting Information). The near single exponential fluorescence decays and, more importantly, wavelength-independent kinetics of the DHI dimers suggest that formation of the radical cation does not occur to a significant extent for any of the dimers studied. The deviation from single exponential decay of the 2,4′-dimer may be a result of conformation or solvent relaxation, but from the fact that all three dimers exhibit kinetics indicative of a single species we expect the decay mechanism to be comparable.

No significant differences in fluorescence dynamics were observed in PVA-containing buffer (Figure 5B), supporting its use as an optimal medium for solution chemistry studies of eumelanin-related species. A different scenario is observed in the case of the glycated dimers, both exhibiting "monomer-like" fluorescence decay (Figure 5C). In particular, two different decay components were observed with 170 and 630 ps lifetimes for gal-DHI 2,7′-dimer and 100 and 760 ps for the 2,4′-isomer (Figure S7, Supporting Information). In both cases the faster component dominated the kinetics at shorter fluorescence wavelengths. The observed differences between the decay dynamics of the DHI dimers and their galactosylthio derivatives, and the appearance in the latter of a fast component reminiscent of the monomer behavior, can be taken to reflect the different structural characteristics of the biindole scaffolds of DHI and gal-DHI. In the former case favorable electronic interaction between the units enabled by favorable planar conformations would lead to altered excited state properties, whereby UV excitation no longer leads to radical formation and the excited state lifetime is on the nanosecond scale. For the gal-DHI dimers, on the other hand, the steric interactions introduced by the bulky sugar groups would force the DHI units to twist out of plane, decreasing π-electron communication between units and accounting for accentuated monomer-like excited state behavior.

Fluorescence Decay Kinetics: Polymers. Fluorescence decay kinetics of the DHI polymer in PVA/buffer and of the gal-DHI polymer in buffer are shown in Figures 6 and 7, respectively. For both samples complete solubilization of the polymers was verified by dynamic light scattering,[21,38,43] implying that excited state dynamics are not affected by aggregation or scattering effects and that issues related to

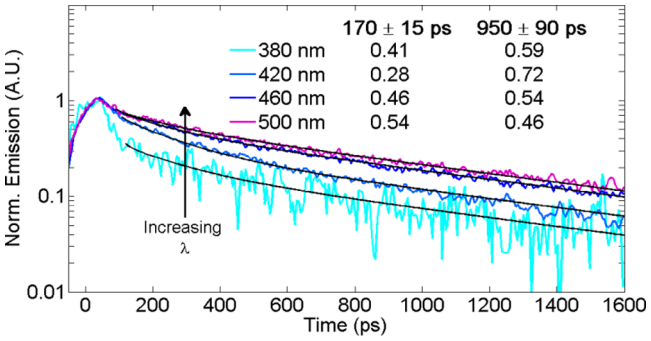

Figure 7. Fluorescence decay kinetics of the gal-DHI polymer in buffer, including fits using a biexponential decay function and the resulting lifetimes. A third unresolved decay is present (less than 10 ps) with uncertain amplitude.

insolubility are satisfactorily settled. Data show that the fluorescence decays of both polymers exhibit a relatively complex behavior, with wavelength-dependent kinetics comprising both nanosecond and picosecond decay components, on account of the expected structural and conformational heterogeneity of the polymers. Although a clear-cut identification of mono- or biexponential decays and detailed interpretation of the kinetic data proved not feasible at this stage and awaits further investigations, some relevant aspects can be briefly discussed here.

The fluorescence decay kinetics for the two soluble polymers are nonexponential in both cases, but more so for the gal-DHI polymer. The DHI polymer solubilized in buffer/PVA solution shows a wavelength-dependent behavior with short-lived decay components (<100 ps) on both the blue and red sides of the fluorescence spectrum, in addition to slow (1.6−3.0 ns) decays (Figure 6 A and B). This behavior suggests the involvement of multiple species, preventing unambiguous interpretation on the basis of the available experimental data. The fast decay on the blue side could possibly be analogous to the 110 ps radical decay of the DHI monomer, but the nature of the long-wavelength (∼480 nm) short-lived decay is unclear at present. The gal-DHI polymer exhibits a fluorescence decay reminiscent of its dimers (Figure 7), though it carries more of the subnanosecond decay on the short-wavelength side of the fluorescence spectrum. It is thus suggested that the apparent monomer/dimer-like behavior is due to steric interactions between the bulky sugar groups causing deviation from coplanarity and reduced electronic interaction between indole units. Further work is required to better understand the origin of the polymer excited state dynamics.

■ CONCLUSIONS

This paper is the first to report picosecond and nanosecond time-resolved data on the excited electronic state dynamics of monomer−dimer−polymer sets of DHI-based model eumelanin systems under scattering-free conditions. Methodological highlights of the present study include the following: (1) use of pristine eumelanin-like polymers of homogeneous monomer composition, to decrease chemical heterogeneity; (2) a solution chemistry approach circumventing scattering effects; (3) complementary strategies for water solubilization based on monomer functionalization and aggregation inhibition by PVA; and (4) use of bulky sugar groups and a sulfur link as a means of disentangling and manipulating excited state decay dynamics.

A schematic outline of the main results summarizing the effects of glycosylation and unit coupling on excited state dynamics is provided in Figure 8.

The key findings emerging from this study are the following: (1) dimerization and polymerization of DHI result in long-lived (nanosecond) excited states with profoundly altered properties relative to the monomer; (2) glycosylation of DHI imparts

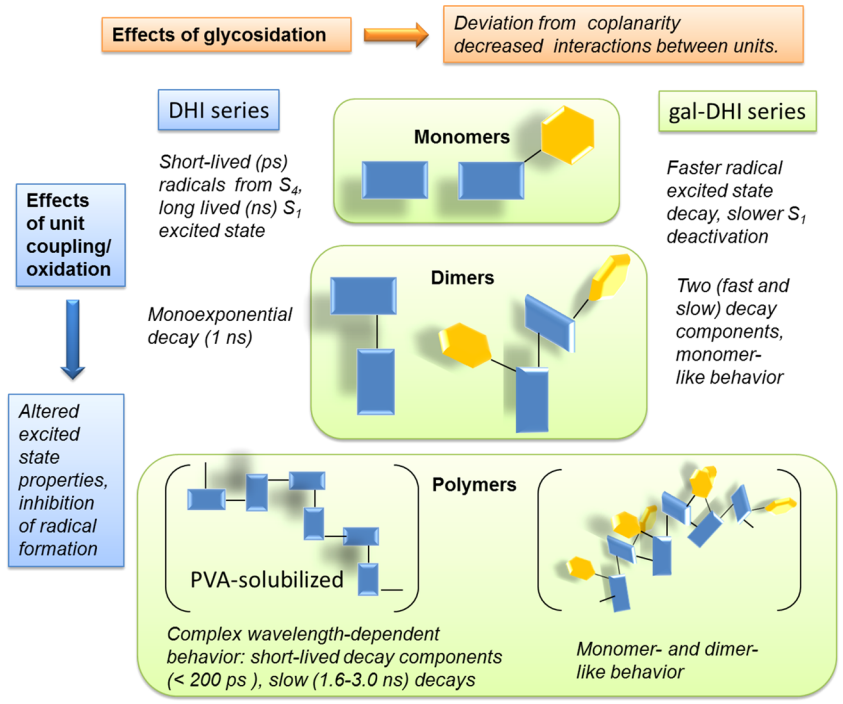

Figure 8. Schematic illustration of the excited state properties of DHI-based monomers, dimers, and polymers and the effects of glycosylation. Conformational properties of the reported species are highlighted.

dx.doi.org/10.1021/jp306436f | J. Phys. Chem. B 2012, 116, 13151−13158

monomer-like behavior to oligomers and polymers, due to steric effects hindering planar conformations and efficient interunit electron communication. These results shed light for the first time on the fundamental emission dynamics of key eumelanin building blocks and model polymers disentangled from aggregation and solid state scattering effects, a finding of possible relevance to eumelanin photoprotection. Moreover, glycosylation is proposed as a valuable means of probing and controlling emission characteristics of eumelanin-like polymers, also in the prospects of developing structurally defined, robust, water-soluble eumelanin-like systems for light harvesting and other possible technological applications.[12]

■ ASSOCIATED CONTENT

Supporting Information

Additional figures of optical absorption spectra, mono- and bi-dimensional plots of fluoresecence decay, and emission spectra and tables of amplitude. This material is available free of charge via the Internet at http://pubs.acs.org.

■ AUTHOR INFORMATION

Corresponding Author

*E-mail: alessandro.pezzella@unina.it.

Present Address

[⊥]Optical Sciences Group, MESA+ Institute for Nanotechnology, University of Twente, 7500 AE, The Netherlands.

Notes

The authors declare no competing financial interest.

■ ACKNOWLEDGMENTS

The work at Lund University was performed with funding from the Swedish Research Council, the Knut&Alice Wallenberg Foundation, the Swedish Energy Agency (STEM), and the European Research Council (Advanced Investigator Grant 226136-VISCHEM). M.d'I. thanks Italian MIUR (PRIN projects) for financial support. A.P. acknowledges support from the European Science Foundation (ESF) for the activity entitled "Ultrafast Structural Dynamics in Physics, Chemistry, Biology and Material Science". The work was supported by European Community under "Laserlab-Europe" Integrated Infrasctructure Programme at the Lund Laser. The project is in the frame of the EuMelaNet programme (http://www.espcr.org/eumelanet/).

■ REFERENCES

(1) Ito, S.; Wakamatsu, K. *J. Eur. Acad. Dermatol.* **2011**, *25*, 1369−1380.

(2) Peles, D. N.; Lin, E.; Wakamatsu, K.; Ito, S.; Simon, J. D. *J. Phys. Chem. Lett.* **2010**, *1*, 2391−2395.

(3) Simon, J. D.; Peles, D.; Wakamatsu, K.; Ito, S. *Pigm. Cell Melanoma Res.* **2009**, *22*, 563−579.

(4) Peles, D. N.; Simon, J. D. *J. Phys. Chem. B* **2011**, *115*, 12624−12631.

(5) Prota, G.; d'Iischia, M.; Mascagna, D. *Melanoma Res.* **1994**, *4*, 351−358.

(6) Panzella, L.; Pezzella, A.; Napolitano, A.; d'Ischia, M. *Org. Lett.* **2007**, *9*, 1411−1414.

(7) d'Ischia, M.; Napolitano, A.; Pezzella, A. *Eur. J. Org. Chem.* **2011**, 5501−5516.

(8) Pezzella, A.; Panzella, L.; Natangelo, A.; Arzillo, M.; Napolitano, A.; d'Ischia, M. *J. Org. Chem.* **2007**, *72*, 9225−9230.

(9) Pezzella, A.; Vogna, D.; Prota, G. *Tetrahedron* **2002**, *58*, 3681−3687.

(10) Pezzella, A.; Vogna, D.; Prota, G. *Tetrahedron: Asymmetry* **2003**, *14*, 1133−1140.

(11) Reale, S.; Crucianelli, M.; Pezzella, A.; d'Ischia, M.; De Angelis, F. *J. Mass Spectrom.* **2012**, *47*, 49−53.

(12) d'Ischia, M.; Napolitano, A.; Pezzella, A.; Meredith, P.; Sarna, T. *Angew. Chem., Int. Ed.* **2009**, *48*, 3914−3921.

(13) Guo, S. L.; Hong, L.; Akhremitchev, B. B.; Simon, J. D. *Photochem. Photobiol.* **2008**, *84*, 671−678.

(14) Schweitzer, A. D.; Howell, R. C.; Jiang, Z. W.; Bryan, R. A.; Gerfen, G.; Chen, C. C.; Mah, D.; Cahill, S.; Casadevall, A.; Dadachova, E. *Plos One* **2009**, *4* (9), e−7229.

(15) Meredith, P.; Sarna, T. *Pigm. Cell Res.* **2006**, *19*, 572−594.

(16) Nighswander-Rempel, S. P.; Mahadevan, I. B.; Rubinsztein-Dunlop, H.; Meredith, P. *Photochem. Photobiol.* **2007**, *83*, 1449−1454.

(17) Tran, M. L.; Powell, B. J.; Meredith, P. *Biophys. J.* **2006**, *90*, 743−752.

(18) Meredith, P.; Powell, B. J.; Riesz, J.; Nighswander-Rempel, S. P.; Pederson, M. R.; Moore, E. G. *Soft Matter* **2006**, *2*, 37−44.

(19) d'Ischia, M.; Crescenzi, O.; Pezzella, A.; Arzillo, M.; Panzella, L.; Napolitano, A.; Barone, V. *Photochem. Photobiol.* **2008**, *84*, 600−607.

(20) Arzillo, M.; Pezzella, A.; Crescenzi, O.; Napolitano, A.; Land, E. J.; Barone, V.; d'Ischia, M. *Org. Lett.* **2010**, *12*, 3250−3253.

(21) Pezzella, A.; Iadonisi, A.; Valerio, S.; Panzella, L.; Napolitano, A.; Adinolfi, M.; d'Ischia, M. *J. Am. Chem. Soc.* **2009**, *131*, 15270−15275.

(22) Nighswander-Rempel, S. P.; Riesz, J.; Gilmore, J.; Bothma, J. P.; Meredith, P. *J. Phys. Chem. B* **2005**, *109*, 20629−20635.

(23) Nighswander-Rempel, S. P.; Riesz, J.; Gilmore, J.; Meredith, P. *J. Chem. Phys.* **2005**, 123.

(24) Simon, J. D. *Acc. Chem. Res.* **2000**, *33*, 307−313.

(25) Liu, Y.; Simon, J. D. *Pigm. Cell Res.* **2003**, *16*, 606−618.

(26) Teuchner, K.; Ehlert, J.; Freyer, W.; Leupold, D.; Altmeyer, P.; Stucker, M.; Hoffmann, K. *J. Fluoresc.* **2000**, *10*, 275−281.

(27) Birch, D. J. S. *Spectrochim. Acta, Part A* **2001**, *57*, 2313−2336.

(28) Forest, S. E.; Simon, J. D. *Photochem. Photobiol.* **1998**, *68*, 296−298.

(29) Meng, S.; Kaxiras, E. *Biophys. J.* **2008**, *95*, 4396−4402.

(30) Olsen, S.; Riesz, J.; Mahadevan, I.; Coutts, A.; Bothma, J. P.; Powell, B. J.; McKenzie, R. H.; Smith, S. C.; Meredith, P. *J. Am. Chem. Soc.* **2007**, *129*, 6672−6673.

(31) Huijser, A.; Pezzella, A.; Sundstrom, V. *Phys. Chem. Chem. Phys.* **2011**, *13*, 9119−9127.

(32) Gai, F.; Rich, R. L.; Petrich, J. W. *J. Am. Chem. Soc.* **1994**, *116*, 735−746.

(33) Gauden, M.; Pezzella, A.; Panzella, L.; Napolitano, A.; d'Ischia, M.; Sundstrom, V. *J. Phys. Chem. B* **2009**, *113*, 12575−12580.

(34) Edge, R.; d'Ischia, M.; Land, E. J.; Napolitano, A.; Navaratnam, S.; Panzella, L.; Pezzella, A.; Ramsden, C. A.; Riley, P. A. *Pigm. Cell Res.* **2006**, *19*, 443−450.

(35) Crippa, P. R.; Giorcelli, C.; Zeise, L. *Langmuir* **2003**, *19*, 348−353.

(36) Gallas, J. M.; Littrell, K. C.; Seifert, S.; Zajac, G. W.; Thiyagarajan, P. *Biophys. J.* **1999**, *77*, 1135−1142.

(37) Ambrico, M.; Ambrico, P. F.; Cardone, A.; Ligonzo, T.; Cicco, S. R.; Di Mundo, R.; Augelli, V.; Farinola, G. M. *Adv. Mater.* **2011**, *23*, 3332−3336.

(38) Pezzella, A.; Ambrogi, V.; Arzillo, M.; Napolitano, A.; Carfagna, C.; d'Ischia, M. *Photochem. Photobiol.* **2010**, *86*, 533−537.

(39) Pezzella, A.; Panzella, L.; Crescenzi, O.; Napolitano, A.; Navaratman, S.; Edge, R.; Land, E. J.; Barone, V.; d'Ischia, M. *J. Am. Chem. Soc.* **2006**, *128*, 15490−15498.

(40) Kaxiras, E.; Tsolakidis, A.; Zonios, G.; Meng, S. *Phys. Rev. Lett.* **2006**, 97.

(41) Sobolewski, A. L.; Domcke, W. *Chemphyschem* **2007**, *8*, 756−762.

(42) Chen, Y.; Liu, B.; Yu, H. T.; Barkley, M. D. *J. Am. Chem. Soc.* **1996**, *118*, 9271−9278.

(43) Arzillo, M.; Mangiapia, G.; Pezzella, A.; Heenan, R. K.; Radulescu, A.; Paduano, L.; d'Ischia, M. *Biomacromolecules* **2012**, *13*, 2379−2390.